Chapter 4

Design of Ligand-Responsive MicroRNAs

This chapter was adapted with permission from Beisel CL, Culler SJ, Hoff KG, and Smolke CD. Design of ligand-responsive microRNAs based on structural insights into Drosha processing. The manuscript was in submission at the time of the thesis defense.

ABSTRACT

MicroRNAs (miRNAs) are endogenous small RNAs that mediate gene silencing in higher eukaryotes and play critical roles in regulating diverse cellular processes. Here, we describe a strategy for engineering ligand-responsive miRNAs in mammalian cells based on structural requirements for efficient Drosha processing – namely, the single-stranded nature of the miRNA basal segments. We utilized a unique property of aptamer binding, termed adaptive recognition, to introduce ligand control over structure within the basal segments, rendering Drosha processing and subsequent gene silencing sensitive to ligand concentrations. The generality of this strategy as a means of introducing ligand control over gene silencing was demonstrated for three different aptamer-small molecule ligand pairs. Furthermore, we explored the versatility of ligand-responsive miRNAs through the engineering of miRNA clusters, cis-acting miRNAs, and self-targeting miRNAs that combine cis and trans regulation. This versatility is an important property for tailoring genetic regulatory systems to applications in biotechnology and medicine that require finely tuned, combinatorial control of transgene or endogenous gene expression. Finally, our synthetic ligand-responsive miRNAs suggests an as yet undiscovered regulatory mechanism for small molecule control of natural miRNAs.

INTRODUCTION

miRNAs comprise a conserved class of small noncoding RNAs that direct targeted gene silencing through the RNA interference (RNAi) pathway in humans and other eukaryotes (Bartel, 2004). Most miRNAs are encoded within long transcripts transcribed from Pol II promoters (Cai *et al*, 2004; Lee *et al*, 2002). The primary (pri-) miRNA is initially processed to an ~65 nucleotide (nt) precursor (pre-)miRNA by the Microprocessor (Gregory *et al*, 2004; Han *et al*, 2004; Lee *et al*, 2003) composed of the cleaving enzyme Drosha and the RNA binding protein DGCR8. Following pri-miRNA cleavage and export from the nucleus, the pre-miRNA is processed by Dicer to a 22-25 nt miRNA duplex. One of the duplex strands termed the mature miRNA is incorporated into the RNA-induced silencing complex (RISC), which subsequently cleaves or translationally represses the target transcript depending on the degree of complementarity between the guide sequence of the miRNA and the target. miRNA-mediated gene regulation has been implicated in diverse biological processes ranging from development to angiogenesis and may be involved in the regulation of a majority of the human genome (Friedman *et al*, 2009).

Engineered genetic systems that display ligand control of gene silencing mediated by miRNAs will provide a powerful and versatile means to control transgene and endogenous gene expression. In addition, the application of such control systems to natural miRNAs will allow coordinated regulation of potentially hundreds of genes and diverse cellular functions (Baek *et al*, 2008; Selbach *et al*, 2008). Recently, researchers have designed synthetic RNA-based regulatory systems that integrate sensing and gene-regulatory functions, where the former are encoded in RNA aptamer sequences that

recognize small molecule ligands (Suess and Weigand, 2008). Such integrated ligand-responsive RNA-based control systems offer several advantages over more traditional protein-based regulatory systems in avoiding potential immunogenicity of heterologous protein components and providing a more tunable control system. In addition, as aptamers can be selected against a wide range of biomolecules (Ellington and Szostak, 1990; Osborne and Ellington, 1997; Tuerk and Gold, 1990), such integrated RNA systems provide platforms for gene expression control in response to potentially any molecular input.

Recently, integrated RNA-based control systems that mediate gene silencing through the RNAi pathway in response to small molecule ligands were built from gene regulatory functions encoded by intermediate substrates in the processing pathway, small hairpin RNAs (shRNAs) (An *et al*, 2006; Beisel *et al*, 2008). The ligand-responsive shRNA system designs linked small molecule RNA aptamers to shRNA elements to modulate the extent of Dicer processing and subsequent gene silencing through ligand binding events based on known structural requirements for efficient Dicer processing (An *et al*, 2006; Beisel *et al*, 2008). However, sequence restrictions and in vivo toxicity of shRNAs (Boudreau *et al*, 2009; Grimm *et al*, 2006; McBride *et al*, 2008) establish significant hurdles toward broader implementation of these control systems. Recent research indicates that such practical application issues may be avoided through the implementation of integrated ligand-responsive miRNAs (Bauer *et al*, 2009; Boudreau *et al*, 2009; McBride *et al*, 2008).

We have designed ligand-responsive miRNAs and demonstrated their implementation in regulatory circuits that modulate and tune the resulting regulatory

response. Our design is based on elucidated structural requirements for miRNA processing, specifically that the bulge size in the miRNA basal segments dictates the extent of Drosha processing and in vivo silencing. By integrating an aptamer into the miRNA basal segments, we utilized aptamer-ligand binding interactions to increase the local structure in that region, such that Drosha processing and subsequent gene silencing were inhibited with increasing ligand concentration. The sequence flexibility of the basal segments allows for the introduction of different aptamer sequences in this region, resulting in a modular design framework that allows modification of the detected ligand or target gene without compromising regulatory activity. We further engineered circuits comprising clusters of ligand-responsive miRNAs, where the use of cis- or trans-acting miRNAs at variable copy number provided tunable control of gene expression. We also engineered a self-targeting ligand-responsive miRNA circuit based on combined cis and trans regulation that resulted in more stringent regulatory properties, providing a novel system for transgenic control. Our integrated ligand-responsive miRNA framework offers considerable versatility for genetic control and will be broadly useful across applications in biotechnology and medicine.

RESULTS

Extent of structure in the basal segments dictates Drosha processing and gene silencing

miRNAs can be partitioned into four domains (Figure 4.1A) that exhibit unique structural requirements for efficient Drosha processing and RISC activation (Boudreau *et al*, 2008; Han *et al*, 2006; Zeng and Cullen, 2003, 2004, 2005; Zeng *et al*, 2005). For

example, in vitro studies have shown that mutating the sequence of the basal segments to form extensive base pairing interactions abolishes Drosha processing (Han *et al*, 2006; Zeng and Cullen, 2005). These results indicate that efficient Drosha processing requires that the basal segments be single-stranded or unstructured.

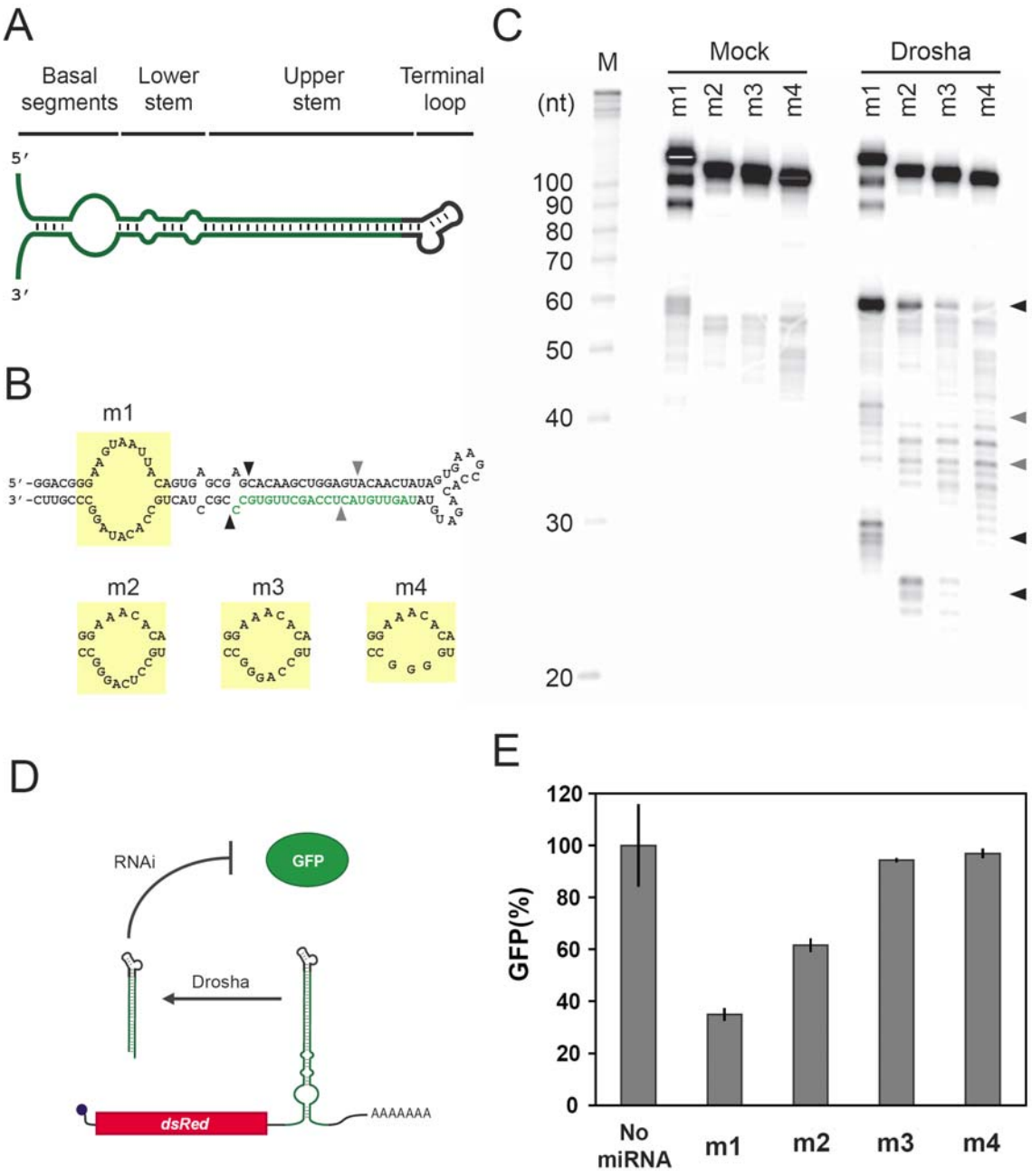

Figure 4.1 Extent of structure in the basal segments dictates miRNA processing and target gene silencing. (**A**) General domains of a pri-miRNA. The upper stem encodes the mature miRNA sequence. The lower stem is ~11 base pairs (bp) in length and designates the Drosha cleavage site. The basal segments comprise the flanking sequences outside of the lower stem. (**B**) Sequence and secondary structures of minimal pri-miRNAs used to examine the effects of bulge size in the basal segments on Drosha processing in vitro. The minimal pri-miRNAs contain a mature miRNA sequence that targets GFP (green text) and differ only in their basal segments. The bulge sequences for each pri-miRNA are indicated in yellow boxes. Black and gray arrows indicate the putative cleavage sites for productive and abortive processing, respectively, based on data from the cleavage assay. (**C**) In vitro Drosha cleavage assay results on the minimal pri-miRNAs with varying bulge sizes. Internally radiolabeled miRNAs were incubated with immunopurified Drosha (Drosha) or mock preparations (Mock), and reaction products were resolved by PAGE. Productive processing is expected to result in an ~61 nt pre-miRNA. Black and gray arrows mark the presumed productive and abortive cleavage products, respectively, from Drosha cleavage as indicated in (B). Gel images are representative of at least two independent experiments. (**D**) Schematic of the in vivo miRNA expression and targeting system. GFP-targeting miRNAs were placed within the 3' UTR of a transcript encoding DsRed-Express that was expressed from the constitutive CMV promoter. (**E**) GFP silencing results from cell culture assays performed with miRNAs exhibiting varying bulge sizes. The population median of GFP fluorescence from transiently transfected HEK 293 cells stably expressing GFP was normalized to that from a construct lacking a miRNA (No miRNA). Error bars represent the standard deviation of two independent transfections.

This requirement suggests a mechanism for regulating Drosha processing, and thus RNAi-mediated gene silencing, by regulating the structure of the basal segments. To utilize this mechanism as a design strategy, we more systematically examined the relationship between bulge size in the miRNA basal segments, in vitro Drosha processing, and in vivo gene silencing.

We performed in vitro Drosha cleavage assays that mimic the first step in miRNA biogenesis to examine the relationship between bulge size and Drosha processing. RNAs with varying bulge sizes in the basal segments (Figure 4.1B) were transcribed in vitro, incubated with immunopurified Drosha, and resolved by PAGE (Figure 4.1C). Decreasing the size of the loop from 18 to 8 nts greatly reduced the appearance of the 61 nt pre-miRNA (Figure 4.1B, black arrows) and increased abortive processing (Figure 4.1B, gray arrows). Abortive processing was previously observed and attributed to DGCR8 recognition of the terminal loop instead of the miRNA basal segments (Han *et al*, 2006).

To examine the relationship between bulge size in the basal segments and gene silencing, we developed a general cell culture assay for miRNA activity (Figure 4.1D). miRNAs designed to target a transcript encoding the green fluorescent protein (GFP) were inserted into the 3' untranslated region (UTR) of a constitutively-expressed transcript encoding the fluorescent protein DsRed-Express. Plasmid DNA encoding the DsRed-Express construct was transfected into HEK 293 cells stably expressing GFP. The level of miRNA-mediated gene silencing was determined by flow cytometry analysis, where DsRed-Express levels were used to distinguish between transfected and untransfected cells. Using the cell culture assay, miRNAs with the same bulges as in the

in vitro experiments were tested for silencing efficiency. Flow cytometry results supported the data from the in vitro Drosha cleavage assays, as smaller bulge sizes showed reduced GFP silencing (Figure 4.1E). Therefore, proper Drosha processing and gene silencing correlate with the size of the bulge in the miRNA basal segments.

Aptamer integration renders miRNA processing sensitive to a small molecule ligand

Aptamers often undergo transitions from unstructured to highly structured conformations upon ligand binding, a phenomenon termed adaptive recognition (Hermann and Patel, 2000). We developed a design strategy based on this phenomenon and the dependence of Drosha processing on the structure of the basal segments to introduce ligand control of miRNA-mediated gene silencing (Figure 4.2A). Through integration of an aptamer into the basal segments of a miRNA, we anticipated that the aptamer-ligand binding interactions would decrease the unstructured nature of that region, thereby inhibiting proper processing and subsequent gene silencing (Figure 4.2B).

We first examined the ability of an aptamer to mediate ligand control of Drosha processing. The theophylline aptamer (Jenison *et al*, 1994; Zimmermann *et al*, 2000) was inserted in the basal segments domain directly adjacent to the miRNA lower stem (Figure 4.2C). The resulting miRNA (th1) was transcribed in vitro and subjected to the Drosha cleavage assay in the presence or absence of theophylline. The primary products of Drosha processing for th1 and a control miRNA were both ~61 nts, the expected size for the pre-miRNA (Han *et al*, 2006; Lee *et al*, 2003) (Figure 4.2D). In addition, the presence of theophylline inhibited proper processing of the aptamer-containing miRNA, resulting in an alternative cleavage pattern similar to that observed from miRNAs with smaller

bulges (Figure 4.1C). The control miRNA exhibited negligible theophylline dependence, suggesting that ligand binding to an aptamer located within the basal segments can control Drosha processing.

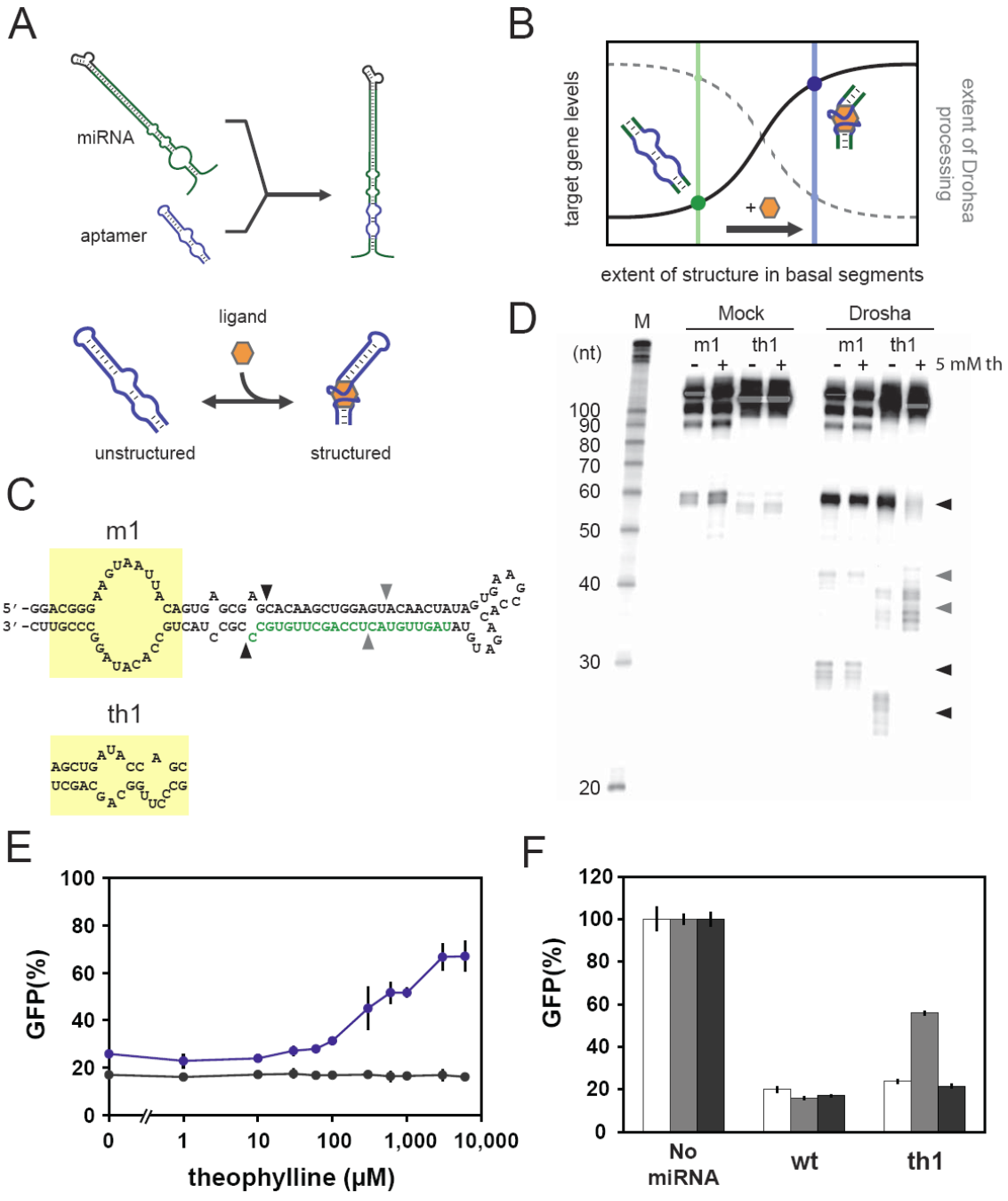

Figure 4.2 Ligand-responsive miRNAs enable ligand-mediated regulation of Drosha processing and gene silencing. (**A**) A design framework for ligand-responsive miRNAs based on integrating the aptamer binding core into the miRNA basal segments directly adjacent to the lower stem. Drosha processing of the miRNA is inhibited through an increase in structure of the basal segments domain resulting from the binding interaction between the aptamer and its cognate ligand. (**B**) Proposed relationship between Drosha processing (dashed gray line), target gene expression levels (black line), miRNA basal segments structure, and ligand concentration for a ligand-responsive miRNA. Unstructured basal segments lead to efficient processing and gene silencing, whereas structured basal segments, resulting from ligand binding and favored as the ligand concentration increases, inhibit Drosha processing. (**C**) Sequence and secondary structures of minimal GFP-targeting pri-miRNAs with a large bulge (m1) or the theophylline aptamer (th1) inserted in the basal segments. Notation follows that indicated in Figure 4.1B. (**D**) In vitro Drosha cleavage assay results for m1 and th1. Internally radiolabeled miRNAs were incubated with immunopurified Drosha (Drosha) or mock preparations (Mock) in the presence or absence of 5 mM theophylline, and reaction products were resolved by PAGE. Black and gray arrows mark the presumed productive and abortive cleavage products, respectively, from Drosha cleavage as indicated in (**c**). Gel images are representative of at least two independent experiments. (**E**) Theophylline response curves for constructs harboring a GFP-targeting miRNA with basal segments containing the theophylline aptamer (th1, blue) or sequence similar to miR-30a (wt, gray) (Figure S4.1). miRNAs were cloned into the plasmid constructs and characterized through the cell culture assays described in Figure 4.1D. The population median of GFP fluorescence from transiently transfected HEK 293 cells stably expressing GFP was normalized to that from a construct lacking a miRNA (No miRNA) at each theophylline concentration. wt was used as a negative control as it results in similar levels of GFP silencing in the absence of theophylline. (**F**) GFP silencing results from cell culture assays performed on th1 and wt transiently transfected in the absence (white) or presence of either 5 mM theophylline (gray) or 1 mM caffeine (black).

GFP levels were normalized to that from a construct lacking a miRNA (No miRNA) transfected under the same conditions. Error bars represent the standard deviation of two independent transfections.

We next examined whether theophylline regulation of Drosha processing resulted in ligand-mediated control of gene silencing. Using the cell culture assay, we tested the silencing efficiency of a GFP-targeting miRNA with a theophylline aptamer in the basal segments (th1). Extensive base pairing below the bulge encoded in the aptamer sequence was incorporated to ensure proper aptamer folding. We also included a GFP-targeting miRNA with basal segments similar to the natural miRNA miR-30a as a control (wt, Figure S4.1). Transient transfections were conducted in the presence of varying concentrations of theophylline. Results show that both miRNA constructs silence GFP with comparable strength in the absence of theophylline (Figure 4.2E). However, the miRNA with the theophylline aptamer mediated a theophylline dose-dependent increase in GFP expression levels, whereas silencing by the miRNA lacking the aptamer was insensitive to theophylline. In addition, silencing by both miRNAs was insensitive to the presence of caffeine (Figure 4.2F), a molecule that differs from theophylline by a single methyl group and binds the theophylline aptamer with a 10,000-fold lower affinity (Jenison *et al*, 1994). The results demonstrate that the observed effect of theophylline on miRNA-mediated gene silencing is specific to the incorporation of the theophylline aptamer in the basal segments of the miRNA.

Framework modularity supports the integration of different aptamer and miRNA targeting sequences

A desirable property of any ligand-responsive regulatory system is modularity. Modular regulatory systems can be readily modified to change the targeted gene or recognized ligand without complete redesign, facilitating the rapid implementation of base designs in diverse applications with varying regulatory needs. While most ligand-responsive RNA regulator designs can be readily modified to target different genes, only a fraction of the developed designs have been shown to support direct insertion of different aptamer sequences (Bayer and Smolke, 2005; Beisel *et al*, 2008; Win and Smolke, 2007).

The targeted gene is specified by the mature miRNA sequence in a miRNA regulatory element. Previous work has shown that modifying the mature miRNA sequence in natural miRNAs is sufficient to target different genes (Zeng *et al*, 2002). Since the aptamer and mature miRNA sequences do not overlap, we expected that each of these elements can be changed independently without affecting the other's function. Using the cell culture assay, we tested two different mature miRNA sequences: one that targets a different location in the GFP encoding transcript (th2) and the other that is partially scrambled (th1'). Flow cytometry results showed GFP silencing and theophylline-dependent up-regulation of gene expression by th2 and negligible silencing by th1' (Figure S4.2). Therefore, the mature miRNA sequence can be modified without compromising the ligand control function encoded within the aptamer sequence.

To examine the modularity of the aptamer sequence, we tested two aptamers that display different lengths and secondary structures: the tetracycline aptamer (Berens *et al*,

2001) and the xanthine aptamer (Kiga *et al*, 1998). The binding core of each aptamer was initially integrated adjacent to the lower stem in place of the bulge (Figure 4.3A), and the resulting miRNAs were tested using the cell culture assay in the presence or absence of the associated ligand. Hypoxanthine was used as a soluble alternative to xanthine that binds the aptamer with comparable affinity (Kiga *et al*, 1998). Control miRNAs that resulted in similar levels of gene silencing as the ligand-responsive miRNAs in the absence of ligand were also tested to determine any non-specific impacts of ligand addition on GFP levels. The miRNA harboring the tetracycline aptamer (tc1) down-regulated GFP and mediated a tetracycline-dependent increase in GFP levels (Figure 4.3B). The control miRNA (m2) delivered a similar extent of silencing with negligible tetracycline dependence, indicating that insertion of the tetracycline aptamer rendered gene silencing sensitive to tetracycline. However, compared to the theophylline aptamer, insertion of the tetracycline aptamer imparted reduced silencing and ligand sensitivity. The altered silencing in the absence of ligand may be attributed to the nature of the unbound aptamer structure, where the tetracycline aptamer folds into a preformed pocket (Muller *et al*, 2006). The altered regulatory response may be attributed to aptamer affinity, the relative membrane permeability of each small molecule, and the extent to which each aptamer adopts a more structured conformation upon ligand binding.

In contrast, insertion of the binding core of the xanthine aptamer (xa1) completely abolished silencing (Figure 4.3C). The size of the bulge in the basal segments of xa1 was similar to m4, the miRNA with the smallest bulge tested (Figure 4.1B), such that the small size of the xanthine binding core may similarly prevent proper Drosha processing. We speculated that an aptamer with a small binding core bulge can be made more

unstructured by including additional bulges, thereby restoring proper processing. Most aptamers selected in vitro contain loops that are separate from the binding core. To decrease the structure of the basal segments without compromising binding activity, we included the loop of the original xanthine aptamer and inverted the aptamer sequence to ensure hypoxanthine binding was proximal to the lower stem (xa2). Results from the cell culture assay showed significant GFP silencing and a hypoxanthine-dependent increase in GFP levels (Figure 4.3C), whereas hypoxanthine had no effect on a control miRNA with a similar silencing strength (m1). To further probe the specificity of ligand dependence, we repeated the cell culture assays using tc1 or xa2 with tetracycline or hypoxanthine. Results showed that GFP levels increased only when each aptamer was paired with its associated ligand (Figure 4.3D).

Engineering ligand-responsive miRNA clusters for tunable genetic control

Multiple miRNAs can be naturally found in clusters within a single transcript, such as miR-17-92 (He *et al*, 2005) and miR-34b-34c (He *et al*, 2007). Each miRNA within a cluster is individually processed such that cells can efficiently regulate multiple miRNAs through a single promoter. This property provides a level of regulatory efficiency that is currently unavailable to shRNAs, which must be paired with individual promoters to increase copy number (Gonzalez *et al*, 2005) or achieve combinatorial control (Beisel *et al*, 2008). By integrating multiple miRNAs into the same transcript, researchers have exploited this architecture to target multiple genes or tune gene silencing (Aagaard *et al*, 2008; Sun *et al*, 2006; Xia *et al*, 2006). Integrating ligand-responsive

miRNAs into clusters would allow tuning of the regulatory response, simultaneous regulation of different targets, and multi-input control.

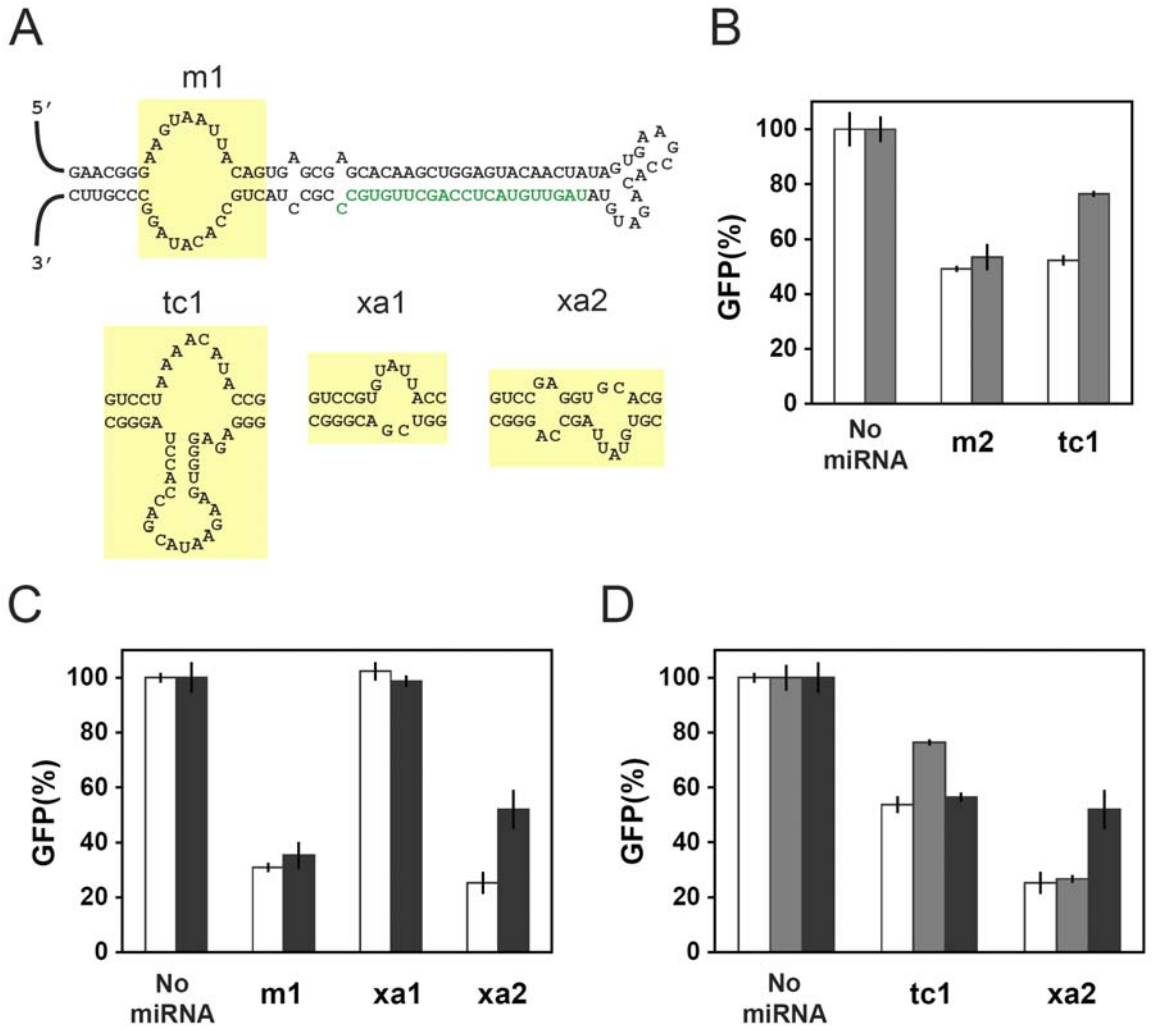

Figure 4.3 Ligand-responsive miRNAs can accommodate different aptamers to tailor the input-responsiveness of the regulatory system. (**A**) Sequence and secondary structures of GFP-targeting pri-miRNAs with the tetracycline (tc1) or xanthine (xa1, xa2) aptamers inserted in the basal segments. The aptamer binding core was inserted for tc1 and xa1, whereas the binding core and loop were inserted for xa2. Notation follows that indicated in Figure 4.1B. (**B-D**) GFP silencing

results for tetracycline- (tc1) and hypoxanthine-responsive (xa1, xa2) miRNA constructs transiently transfected in the absence (white) or presence of either 100 μM tetracycline (gray) or 5 mM hypoxanthine (black). The GFP-targeting miRNAs were cloned into the plasmid constructs and characterized through the cell culture assays described in Figure 4.1D. The population median of GFP fluorescence from transiently transfected HEK 293 cells stably expressing GFP was normalized to that from a construct lacking a miRNA (No miRNA) transfected under the same conditions. m1 and m2 were used as negative controls as they result in similar levels of GFP silencing as xa2 and tc1, respectively, in the absence of ligand. Error bars represent the standard deviation of two independent transfections.

Natural miRNAs in clusters range from being directly adjacent to one another (He *et al*, 2005) to being separated by hundreds of nucleotides (He *et al*, 2007). The variability in spacing may be important in Drosha processing and gene silencing, although the effect of spacing on miRNA activity has not been assessed to date. Therefore, we examined the relationship between the spacer length connecting two ligand-responsive miRNAs and the resulting gene silencing and ligand control. We inserted a second copy of the theophylline-responsive, GFP-targeting miRNA (th1) upstream from the first copy in the 3' UTR of the transcript encoding DsRed-Express with different spacer lengths (Figure 4.4A) and performed the cell culture assay with theophylline. To keep the local sequence around each miRNA consistent, the spacer sequences were identical to the sequence downstream of the first miRNA up to the poly(A) signal. Spacer lengths were measured between the bottoms of each stem below the aptamer and ranged from 2 to 112 nt. Adjacent placement of the miRNAs compromised both silencing and the response to theophylline potentially due to disrupted

miRNA folding or steric hindrance of Drosha processing, whereas increased spacer length restored and even exceeded the silencing activity and theophylline-dependence from a single copy (Figure 4.4B). The results suggest that separating the identical miRNAs a minimal distance improves processing and gene silencing.

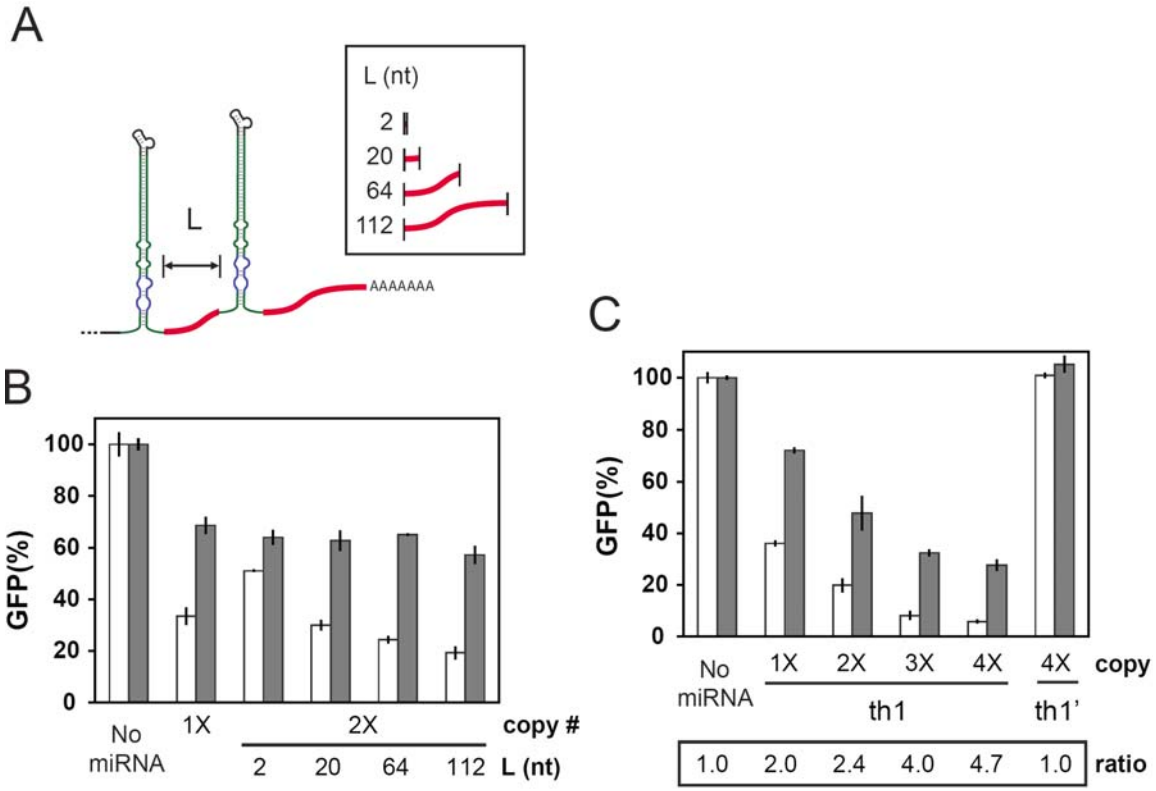

Figure 4.4 Synthetic ligand-responsive miRNA clusters allow tuning of the regulatory response. (**A**) Schematic of a synthetic miRNA cluster in which multiple ligand-responsive miRNAs are placed in the 3' UTR of a transgene encoding transcript. The spacer sequence downstream of each miRNA (indicated in red) was kept consistent, and the spacer length (L) was varied between 2 and 112 nts. Multiple copies (from 1 to 4) of a single miRNA were sequentially inserted. (**B**) The impact of spacer length between two theophylline-responsive GFP-targeting miRNAs (2X,

th1) on gene silencing in the presence (gray) or absence (white) of 5 mM theophylline. The GFP-targeting miRNAs were cloned into the plasmid constructs and characterized through the cell culture assays described in Figure 4.1D. GFP levels are reported as described in Figure 4.3. The GFP silencing from a single-copy theophylline-responsive miRNA construct (1X, th1) is shown for comparison. (**C**) The impact of ligand-responsive miRNA copy number on gene silencing and dynamic range. Multiple copies (#X) of the GFP-targeting (th1) or non-targeting (th1', Figure S4.2) theophylline-responsive miRNAs were cloned into the plasmid constructs described in Figure 4.1D using the largest spacer length tested (112 nt). GFP levels were characterized and reported as described in (B), and the dynamic range is reported as the ratio of GFP levels in the presence and absence of theophylline.

Gene silencing and the dynamic range increased when two copies of a ligand-responsive miRNA were separated by the longest spacer tested (112 nt). As miRNAs in natural clusters are individually processed, we expected that inserting additional copies separated by appropriate spacer lengths would further improve silencing and the theophylline response. Constructs harboring up to four copies of the theophylline-responsive, GFP-targeting miRNA (th1) or four copies of the non-targeting variant (th1') separated by the longest spacer sequence were subjected to the cell culture assay. GFP silencing increased with each additional copy of th1, whereas four copies of th1' had no effect on GFP levels (Figure 4.4C). The addition of each miRNA copy provided more miRNAs for Drosha processing, resulting in greater production of mature miRNAs. The presence of additional miRNA copies also increased the number of opportunities to inhibit Drosha processing, thereby increasing the dynamic range (measured as the ratio between the expression activity in the presence and absence of theophylline).

Therefore, changing the copy number of ligand-responsive miRNAs provides one approach to coordinately tune gene silencing and the dynamic range. The diminished GFP levels in the presence of theophylline may be attributed to the inability to access higher theophylline concentrations due to cytotoxicity (Beisel and Smolke, 2009) and incomplete inhibition of Drosha processing when theophylline is bound to the aptamer.

Ligand-responsive miRNA clusters can regulate endogenous genes

Most of the synthetic ligand-responsive RNA-based regulatory systems are encoded in the target transcript, providing regulation in cis (Desai and Gallivan, 2004; Ogawa and Maeda, 2008; Suess *et al*, 2004; Suess *et al*, 2003; Thompson *et al*, 2002; Win and Smolke, 2007; Yen *et al*, 2004). However, the regulation of endogenous genes through cis regulatory strategies is currently limiting due to the lack of directed recombination technologies. To test whether ligand-responsive miRNAs provide a trans regulatory strategy for the effective regulation of endogenous genes, we cloned a miRNA that targets the endogenous La gene (La1) into the 3' UTR of a transcript encoding DsRed-Express (Figure 4.5A). Under transient transfection conditions, La1 resulted in only 40% knockdown as measured by qRT-PCR (data not shown). To improve silencing, we cloned four copies of La1 or a La-targeting miRNA harboring the theophylline aptamer (La2) separated by the longest spacer sequence into the 3' UTR of the transcript encoding DsRed-Express. We made HEK 293 stable cell lines with single integrands of these constructs in the same genomic locus to reduce variability in the bulk qRT-PCR measurements. The resulting lines were grown in the presence or absence of theophylline for over one week and assayed for relative La transcript levels by qRT-PCR. Four copies

of either La1 or La2 resulted in relatively strong silencing of the La target, and only La2 mediated a theophylline-dependent increase in La transcript levels (Figure 4.5B). The results demonstrate that ligand-responsive miRNAs can control endogenous genetic targets, providing a control strategy that does not physically disrupt the locus of the target gene.

Ligand-responsive miRNAs can control gene expression in cis

Drosha cleavage separates the pre-miRNA from upstream and downstream sequences. When the miRNA is located in the 3' UTR of a transcript, Drosha cleavage is anticipated to separate the coding region from the poly(A) tail, resulting in the prevention of translation and facilitation of mRNA degradation (Dreyfus and Regnier, 2002; Sachs and Varani, 2000). Drosha was recently shown to cleave a naturally-occurring pseudo-miRNA in the transcript of DGCR8 to regulate the activity of the Microprocessor (Han *et al*, 2009). In addition, a recent study showed that introducing a 3' UTR-encoded miRNA down-regulated expression from the transcript harboring the miRNA (Stern *et al*, 2008). As such, transcripts containing 3' UTR-encoded ligand-responsive miRNAs are expected to be down-regulated in a ligand-dependent manner.

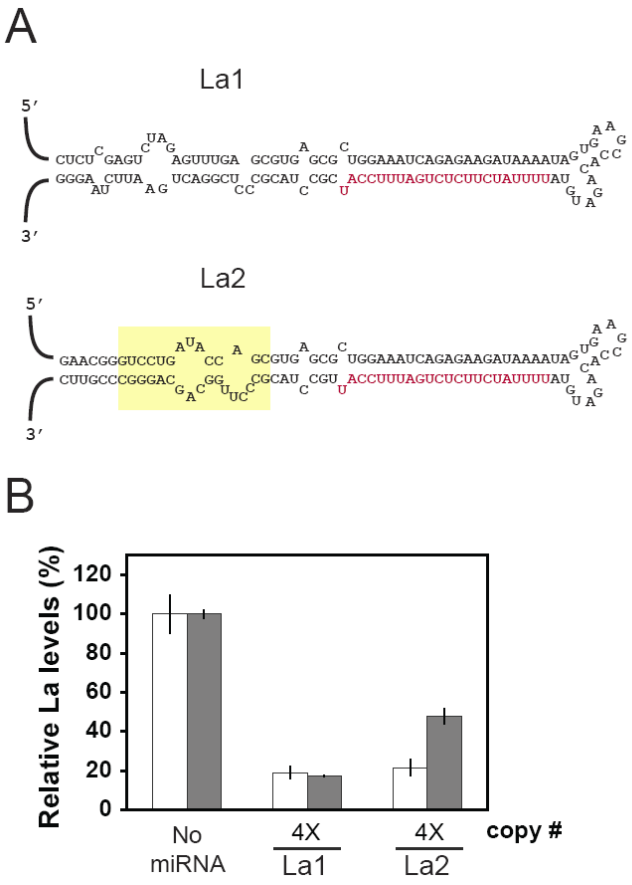

Figure 4.5 Ligand-responsive miRNA clusters can effectively control expression of endogenous gene targets. (**A**) Sequence and secondary structures of miRNAs that target the endogenous La gene. Color schemes are identical to Figure 4.1B, except that the mature miRNA sequence complementary to the La transcript is indicated in red. Sequences similar to miR-30a (La1) or the theophylline aptamer (La2) were inserted into the miRNA basal segments. miRNAs were cloned into the plasmid constructs described in Figure 4.1D at the indicated copy numbers using the largest spacer length tested (112 nt). The resulting constructs were stably transfected into HEK 293-Flp-In cells. (**B**) Relative La transcript levels for stable cell lines expressing the La-targeting miRNA constructs in the presence (gray) or absence (white) of 1.5 mM theophylline. La transcript levels were measured through qRT-PCR and normalized to GAPDH encoding transcript levels as an internal control. Relative levels are normalized to that of cells stably

transfected with the construct lacking a miRNA (No miRNA) grown under the same conditions. Error bars represent the calculated error of quadruplicate qRT-PCR wells of each sample.

To assess the capacity for ligand-responsive miRNAs to regulate gene expression in cis, we measured expression levels for the transcripts harboring the ligand-responsive miRNAs targeting GFP and La. DsRed-Express levels were quantified by flow cytometry under similar conditions as the trans-targeted gene silencing experiments. The effects of increasing copy number of the miRNA on cis regulation were examined for the th1 and th1' series. DsRed silencing increased with increasing copy number of the theophylline-responsive, GFP-targeting miRNA (th1), and two copies were sufficient to introduce ligand regulation (Figure 4.6A). Similar effects were observed with four copies of the non-targeting miRNA (th1'), indicating that transcript silencing and ligand control are independent of downstream processing. Transcript analysis confirmed that the predominant regulatory mechanism of ligand-responsive miRNAs in cis is mRNA destabilization (Figure S4.3). A similar analysis on the stably integrated La-targeting miRNAs indicated that four copies of La1 or La2 resulted in significant DsRed-Express down-regulation (Figure 4.6B). In addition, the miRNA containing the theophylline aptamer (La2) conferred an increase in DsRed levels in the presence of theophylline that was not observed for the construct lacking the theophylline aptamer (La1). These results suggest that ligand-responsive miRNAs can regulate transcripts in cis by modulating Drosha cleavage.

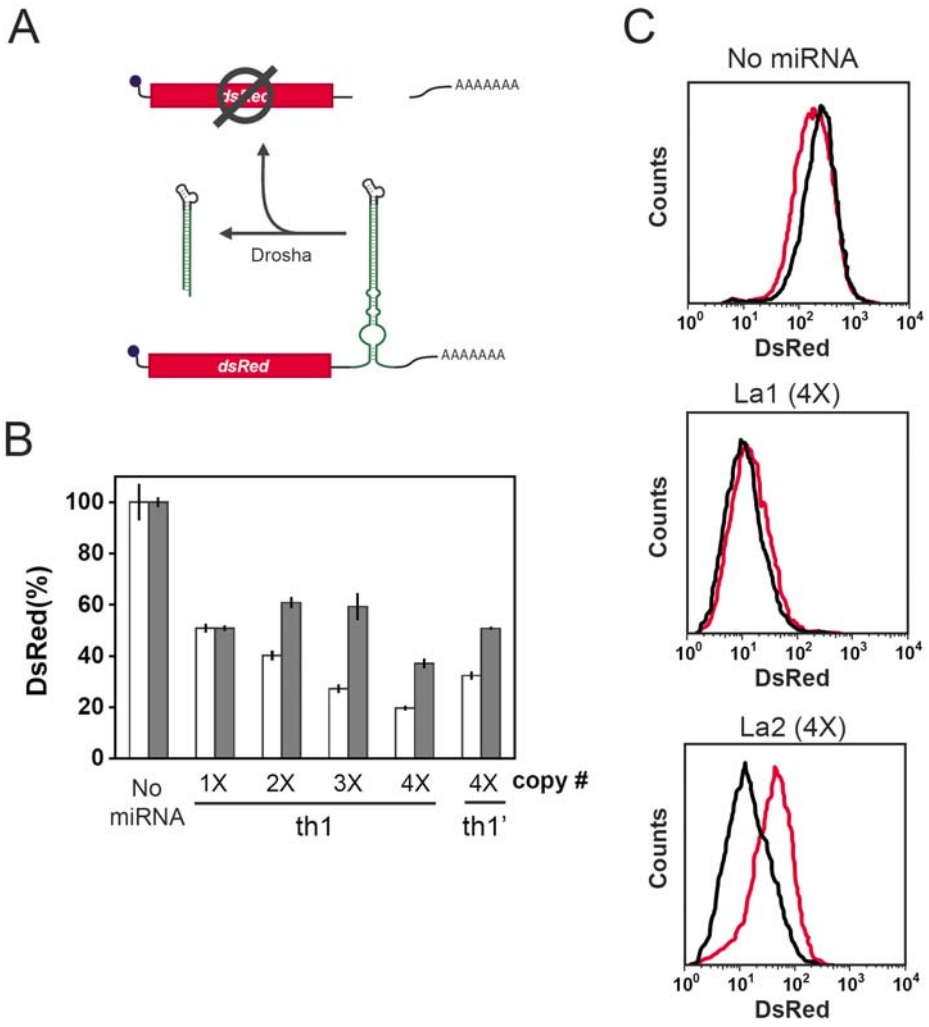

Figure 4.6 Ligand-responsive miRNAs can control transgene expression in cis. (**A**) Schematic of DsRed regulation in cis through miRNA cleavage. Drosha processing of the miRNA located in the 3' UTR separates the coding region from the poly(A) tail, thereby inactivating the transcript. (**B**) The impact of ligand-responsive miRNA copy number on expression of the transgene through regulation in cis in the presence (gray) or absence (white) of 5 mM theophylline. DsRed-Express levels of the constructs tested in Figure 4.4C were characterized through identical cell culture assays. The population mean of DsRed-Express fluorescence from transiently transfected HEK 293 cells stably expressing GFP was normalized to that from a construct lacking any miRNAs (No miRNA) transfected under the same conditions. Error bars represent the standard deviation of

two independent transfections. (**C**) Flow cytometry histograms for DsRed-Express levels from the La-targeting miRNAs. The stable cell lines tested in Figure 4.5B were grown in the presence (red) or absence (black) of 1.5 mM theophylline for over a week prior to flow cytometry analysis. Histograms are representative of two independent experiments.

Self-targeting miRNAs combine trans and cis regulation for a tighter control system

Ligand-responsive miRNAs can regulate genes in trans through RISC targeting and in cis through Drosha cleavage. A control system based on combining both modes of regulation into 'self-targeting miRNAs' may offer tighter regulation while still operating within the 3' UTR of the transgene encoding transcript. We developed a dual-acting miRNA circuit based on the insertion of ligand-responsive miRNAs or miRNA clusters into the 3' UTR of a targeted GFP transcript (Figure 4.7A), where ligand-responsive control of Drosha cleavage is expected to impact direct destabilization of the cleaved transcript and subsequent RISC-mediated inactivation of other target transcripts. The resulting constructs were stably integrated into a single genomic locus in HEK 293 cells to ensure consistent expression for all constructs. Cells were grown in the presence or absence of theophylline for over a week and analyzed by flow cytometry. The self-targeting miRNAs (combined cis and trans mechanism; th1) improved both GFP silencing and the dynamic range as compared to their non-targeting counterparts (cis mechanism; th1') (Figure 4.7B**,** Figure S4.4). Similar effects were observed for the self-targeting miRNA clusters. These results demonstrate the diverse tuning capabilities when encoding ligand-responsive miRNAs in a transcript 3' UTR by implementing self-targeting and non-targeting miRNAs at different copy numbers.

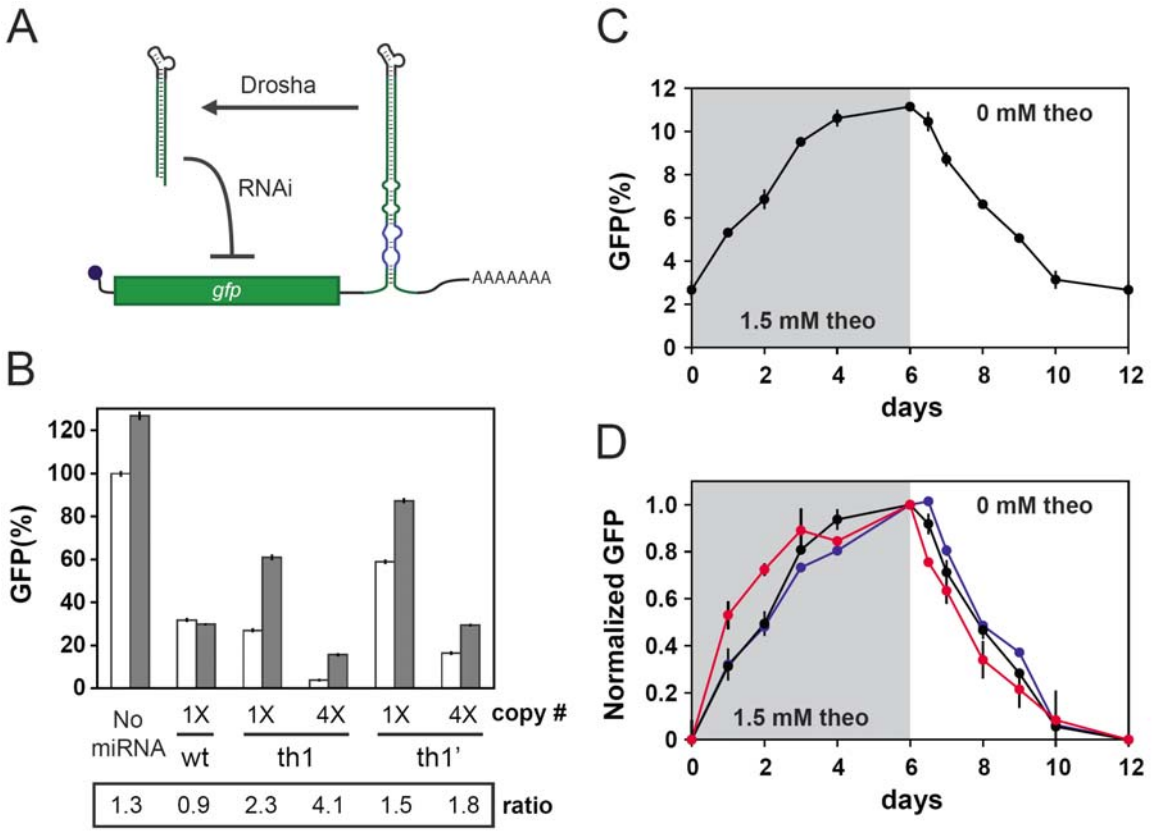

Figure 4.7 Self-targeting miRNAs provide an enhanced regulatory response. (**A**) Schematic of the miRNA regulatory circuit associated with self-targeting miRNAs. Self-targeting miRNAs are located in the 3' UTR of the trans targeted transcript encoding GFP such that Drosha cleavage and RISC targeting down-regulate expression. Both events are inhibited by ligand binding to the aptamer contained in the miRNA basal segments. (**B**) Relative GFP levels for cells stably expressing the self-targeting miRNA constructs grown in the presence (gray) or absence (white) of 1.5 mM theophylline for over a week. Gene silencing from one (1X) or four (4X) copies of a theophylline-responsive self-targeting miRNA (th1) and one or four copies of a theophylline-responsive non-targeting miRNA (th1') were determined, where multiple copies were separated by the largest spacer length (112 nt). One copy of a self-targeting miRNA with basal segments similar to miR-30a (wt) was used as a negative control. The dynamic range is reported as the ratio of GFP levels in the presence and absence of theophylline. (**C**) Temporal response of the relative

GFP levels to a change in ligand concentration for cell lines stably expressing ligand-responsive miRNAs. Representative time course data is shown for cells expressing the miRNA construct containing four copies of th1. Cells were grown in the presence of 1.5 mM theophylline for six days and then transferred to media without theophylline for six days. (**D**) Normalized GFP levels for cell lines stably expressing ligand-responsive miRNAs over time in changing concentrations of ligand. Normalized time course data are shown for cells expressing the miRNA constructs containing four copies of th1' (red), one copy of th1 (blue), or four copies of th1 (black). Time course data were normalized to zero when theophylline was added at the beginning of the time course and one when theophylline was removed in the middle of the time course to compare the dynamics of the approach to steady-state between ligand-responsive miRNAs acting through different regulatory mechanisms. Error bars represent the standard deviation of cells grown in two separate culture wells.

We performed time course studies on the dual-acting miRNA circuits to examine the dynamic properties of these regulatory systems. Cells lines were grown in the presence of theophylline for six days and then grown in media without theophylline for another six days. Cell lines harboring th1 or th1' in single or four copies exhibited increasing GFP levels when grown in the presence of theophylline and reached steady-state levels by day 6 (Figure 4.7C). GFP levels decreased upon removal of theophylline and returned to original levels after 4-6 days of growth in the absence of theophylline, indicating that the genetic control exerted by ligand-responsive miRNAs is reversible.

We further examined the effects of miRNA copy number and regulatory mechanism (cis, dual cis/trans) on the dynamics of the ligand-responsive miRNA regulatory response (Figure 4.7D). Time-course data for th1, th1 (4 copies), and th1' (4

copies) were normalized to lie between zero and one, marking the steady-state levels in the absence or presence of theophylline, respectively. Cells with four copies of the non-targeting miRNA (th1') approached steady-state faster than the self-targeting miRNA (th1), especially upon the addition of theophylline. Cells with either one or four copies of the self-targeting miRNA approached steady state at similar rates. The different rates of approach to steady-state between the non-targeting and self-targeting miRNAs can be explained by the machinery involved in each response. Transcripts harboring the non-targeting miRNAs are regulated directly by Drosha processing, which is rapidly modulated by ligand binding and release. The approach to steady-state is thus set by the rates of transcription and translation when theophylline is added and by GFP turnover and dilution when theophylline is removed. Conversely, transcripts harboring self-targeting miRNAs are regulated by both Drosha processing and subsequent RISC targeting. Therefore, the approach to steady-state levels following theophylline addition is anticipated to be slower since transcript levels will continue to increase after the turnover of activated RISC (Bartlett and Davis, 2006). However, the response to theophylline removal is more similar for non-targeting and self-targeting miRNAs due to the small time lag between Drosha processing and RISC activation in comparison to GFP turnover and dilution. The particular response dynamics associated with the cis and cis/trans regulatory mechanisms offer yet another design parameter when specifying the regulatory performance of ligand-responsive miRNAs.

DISCUSSION

We have developed a novel mode of RNA-based gene regulation in mammalian cells based on synthetic ligand-responsive miRNAs. Ligand-responsive miRNAs function through ligand-mediated regulation of Drosha processing of a pri-miRNA based on modulation of the structured nature of the basal segments region through aptamer-ligand binding interactions. The use of theophylline, tetracycline, and hypoxanthine as effective ligands in this work supports the ability to utilize diverse molecules to control miRNA activity, such as metabolites, metals, and proteins, against which aptamers have been selected (Lee *et al*, 2004). Beyond in vitro selected aptamers, aptamers present in natural riboswitches have also been integrated into RNA-based ligand control systems (Barrick and Breaker, 2007). While most aptamers conform to a standard bulge-loop structure, a significant number adopt alternative structures, such as pseudoknots (Lorsch and Szostak, 1994; Mannironi *et al*, 1997; Tuerk *et al*, 1992; Wilson *et al*, 1998) or dangling ends (Koizumi and Breaker, 2000), that may be incompatible with the ligand-responsive miRNA framework. To address such broader implementation challenges, future work may focus on the development of modified frameworks that accept more diverse aptamer structures, the modification of aptamer selection procedures to preferentially select bulge-loop structures, or the selection of aptamers within RNA-based regulatory systems to identify sequences that function as integrated sensing components (Weigand *et al*, 2008).

We showed that ligand-responsive miRNAs can be readily altered to target different genes by changing the mature miRNA sequence. A future extension of our system will be the incorporation of natural miRNA sequences to exploit natural regulatory networks. Natural miRNAs are key players in diverse cellular processes and

help enact global changes in gene expression by simultaneously targeting hundreds of genes. Therefore, ligand-responsive miRNAs can be directly interfaced with the regulatory architecture controlling complex cellular processes. By implementing ligand-responsive miRNAs that respond to endogenously-expressed molecules, these regulatory molecules will provide a platform for reprogramming cellular state according to the intracellular environment, supporting autonomous approaches to tissue engineering and disease treatment.

We also found that gene silencing and ligand responsiveness were dependent on the spacer length between miRNAs in synthetic miRNA clusters. The variable spacing within natural-occurring miRNA clusters suggests that secondary structure of the intervening sequence may be a key factor in miRNA processability and that spacing may be an evolutionary factor to tune miRNA processing and subsequent gene silencing activity. Future studies that correlate the secondary structures of natural miRNA clusters with the extent of processing of each miRNA will provide further insight into this relationship. From this enhanced understanding, molecular engineers may be able to design synthetic cluster expression platforms that will minimize the cluster length, while maximizing the processing of the encoded miRNAs (Aagaard *et al*, 2008). Scalable synthetic cluster expression platforms will also be important tools in the development of sophisticated gene regulatory circuits based on simultaneous implementation of multiple ligand-responsive miRNAs to achieve finely tuned, combinatorial gene expression control schemes. Such scalable systems will require an understanding of how to engineer molecular platforms that effectively insulate the function of individual miRNA elements within larger clusters and thus an enhanced understanding of RNA structure-function

relationships. However, the practical size of an engineered miRNA cluster may be limited by downstream bottlenecks in the linear pathway of miRNA biogenesis, such as Drosha cleavage, nuclear export, Dicer processing, and RISC loading and targeting.

The linear pathway of miRNA biogenesis offers multiple points at which to engineer ligand-responsive control of RNAi-mediated gene silencing. Besides regulation of Drosha cleavage, RNA-based regulatory frameworks have been reported that regulate nuclear export (Beisel *et al*, 2008) and Dicer processing (An *et al*, 2006; Beisel *et al*, 2008). Since miRNA biogenesis spans the nuclear and the cytoplasmic compartments of the cell, specific regulatory approaches may be more appropriate for a given application depending on the localization properties of the ligand. Furthermore, more sophisticated regulatory strategies can be designed that combine regulatory modes to coordinately modulate multiple points in the processing pathway by integrating aptamers to the same ligand or different ligands.

The synthetic ligand-responsive miRNA systems reported here may foreshadow a prevalent strategy used by natural systems to achieve sophisticated control over miRNA regulatory networks. The successful design of such synthetic systems may suggest relevant architectures to assist in the identification of natural counterparts. Researchers have previously identified mechanisms that modulate miRNA activity based on binding interactions between RNA binding proteins and miRNA loops (Guil and Caceres, 2007) and target sites (Kedde *et al*, 2007), lending further support to the likelihood of an as yet undiscovered natural regulatory strategy based on small molecule control of miRNA activity.

MATERIALS AND METHODS

Plasmid construction. The coding region of DsRed-Express was initially cloned with the consensus Kozak sequence (CGCCACC) into the NheI/XhoI restriction sites of pcDNA3.1(+). pcDNA3.1(+) contains the constitutive CMV promoter upstream of a multicloning site. Ligand-responsive and control miRNAs reported in Table S4.1 were cloned into XbaI/ApaI downstream of each coding region. To construct synthetic miRNA clusters, additional miRNAs were digested with AvrII/XhoI and iteratively inserted into XhoI/XbaI within the miRNA-containing plasmid. For the 2-nt spacer, the second miRNA (th3) was separately prepared and inserted. For all other spacer lengths, the original miRNA was amplified with a common forward primer and a reverse primer that hybridizes different distances downstream of the miRNA: Sp.fwd, 5'-GTTCCTGTAGACGGCTCTC-3'; Sp1.rev, 5'-AATACCTAGGCTGATCAGCGGGTTT-3'; Sp2.rev, 5'-AA TACCTAGGAGGGGCAAACAACAG-3'; Sp3.rev, 5'-AATA CCTAGGAAAGGACAGTGGGAGTG-3'. To make stable cell lines, the coding region of DsRed-Express was replaced with EGFP and the entire transcript was excised with NheI/NsiI and cloned into the same sites in pcDNA5/FRT (Invitrogen). Prior to insertion, the NsiI site was introduced into this plasmid at position 1524 using site-directed mutagenesis. All restriction enzymes and T4 DNA ligase were purchased from New England Biolabs. All constructs were sequence-verified (Laragen).

RNA preparation. Internally radiolabeled RNAs were transcribed *in vitro* from an annealed template containing the T7 promoter (5'-TTCTAATACGACTCACTATA**G**GG-3', where **G** is the first transcribed nucleotide) using the Ampliscribe T7 transcription kit

(Epicentre) according to the manufacturer's instructions with [α-^{32}P]-GTP. Following transcription and DNase treatment, the transcription product was purified through a NucAway clean-up column (Ambion) according to manufacturer's instructions and gel-purified by PAGE.

Drosha cleavage assays. In vitro assays were conducted as described previously (Lee and Kim, 2007). Briefly, the Drosha complex was immunopurified from 293T cells transiently transfected with pCK-Drosha-FLAG and pCK-DGCR8-FLAG (9:1 mass ratio). Two days post-transfection, cells were lysed using M-PER (Pierce) according to the manufacturer's instructions and the resulting supernatant was incubated with Anti-FLAG M2 affinity beads (Sigma Aldrich) for at least 1 hr at 4°C with rotation. The beads were then washed with the lysis buffer (20 mM Tris-HCl pH 8.0, 100 mM KCl, 0.2 mM EDTA) five times and evenly divided for the in vitro assays (two in vitro reactions from a 10 cm transfection dish). Radiolabeled RNAs (~10^5 cpm, 3 µl) were combined with 0.75 µl RNasin (Promega), 3 µl reaction buffer (64 mM $MgCl_2$), 8.25 µl water, and 15 µl immunopurified Drosha complex. After an incubation of 90 min at 37°C, the reaction was terminated with the addition of 0.5 M sodium acetate and 0.02% sodium dodecyl sulfate (SDS), phenol:chloroform extracted, and ethanol precipitated. Samples were then resuspended in 15 µl RNA loading buffer (95% formamide, 0.02% SDS, 0.025% bromophenol blue, 0.025% xylene cyanol FF) and resolved on a 12.5% denaturing polyacrylamide gel. The RNA decades ladder (Ambion) was used as a size marker.

Cell culture and transfection. 293 and Flp-In-293 cells were maintained in DMEM supplemented with 10% FBS at 37°C in a 5% CO_2–humidified incubator. Transient transfections were conducted with Fugene 6 (Roche) according to the manufacturer's instructions one day after seeding. Immediately prior to transfection, the media was supplemented with the appropriate ligand at the specified concentration. The media was replaced two days post-transfection. Three days post-transfection, the cells were trypsinized and subjected to flow cytometry analysis on a Cell Lab Quanta SC MPL (Beckman Coulter) and the resulting data was analyzed using the Flowjo software (Tree Star). Cells were initially gated for viability by electronic volume and side scatter. GFP and DsRed fluorescence of viable cells were measured through a 525 nm and 760 nm band pass filter, respectively, after excitation with a 488 nm laser. Moderate to high DsRed levels served as a transfection control to gate between transfected and untransfected cells. Transfected cells could be distinguished from untransfected cells even when four miRNAs were present in the 3'UTR of the DsRed-Express encoding transcript (data not shown). GFP levels were calculated as the median fluorescence of the transfected population divided by that of the untransfected population (Beisel *et al*, 2008). All ratios were normalized such that the value for DsRed-Express lacking a miRNA under the same conditions was set to 100%. Reported DsRed measurements are the mean value of the transfected population normalized to the construct lacking a miRNA set to 100%, where the mean value was selected based on the high variability associated with transient plasmid-based expression of fluorescent proteins.

Stable transfection of 293-Flp-In cell lines was performed using the Flp-In recombinase system (Invitrogen) according to the manufacturer's instructions to generate

isogenic stable cell lines. Integrands were selected using 200 μg/ml hygromycin B (Invitrogen), whereas stable cell lines were maintained in 50 μg/ml hygromycin B. The procedure described above for the fluorescence expression analysis of transiently transfected cell populations was used to analyze the stable cell lines with notable exceptions. Normalization of flow cytometry data to untransfected cells was not performed as all cells express the integrated construct, and all data was normalized to cells lacking a miRNA and grown in the absence of theophylline. Normalization to cells grown under the same conditions was not performed since theophylline differentially affected the two negative controls: no miRNA and a self-targeting miRNA lacking the theophylline aptamer. The different effects may be attributed to differences in perturbations induced by theophylline stress on unregulated genes and genes regulated by a self-targeting miRNA as observed for other cellular stressors (Figure S4.5).

qRT-PCR. The following oligos were used for qRT-PCR. La protein (Acc # X13697): La_fwd, 5'-GGTTGAACCGTCTAACAACAG-3'; La_rev, 5'-ATGTCATCAAGAGTTGCATCAG-3'; GAPDH (Acc # NM_002046): GAPDH_fwd, 5'-GAAGGTGAAGGTCGGAGTC-3'; GAPDH_rev, 5'-GAAGATGGTGATGGGATTTC-3'; DsRed-Express: DsRed.fwd, 5'-AAGAAGACTATGGGCTGGGA-3'; DsRed.rev 5'-CGATGGTGTAGTCCTCGTTG-3'; and the Neomycin resistance gene: NeoR.fwd, 5'-ACCTTGCTCCTGCCGAGAAAGTAT-3'; NeoR.rev, 5'-ATGTTTCGCTTGGTGGTCGAATGG-3'. Transcript levels were measured by qRT-PCR under either transient or stable transfection conditions. For transient transfections 293 cells were washed with 1X PBS three days post-transfection and total RNA was extracted using the RNeasy Mini kit (Qiagen)

according to the manufacturer's instructions. For stable transfections, cell lines were grown for over a week in the presence or absence of 1.5 mM theophylline prior to total RNA extraction. Total RNA samples were treated with DNase I at 37°C for 20 minutes and purified using a NucAway column (Ambion). Up to 5 μg of purified RNA was reverse-transcribed using Superscript III reverse transcriptase (Invitrogen) according to the manufacturer's instructions using the reverse primers for each pair of gene target and loading control (DsRed/NeoR, La/GAPDH) followed by the recommended incubation with RNase H. qRT-PCR was conducted with the resulting cDNA on the iCycler iQ system (BioRAD) according to the manufacturer's instructions. Samples were prepared in quadruplicate using the iQ SYBR green supermix and data were analyzed using the iCycler iQ software. The mean of the resulting C_T values for the target gene of each sample were subtracted from the mean C_T value for the control gene. The resulting values were then converted from $\log_2$ to linear scale and normalized to the value for the sample lacking any miRNA transfected with the same concentration of ligand. The reported sample error was calculated using the following expression:

$$\text{Sample Error} = \frac{2^{\text{AVE(Cont)}-\text{AVE(Target)}+\frac{1}{2}[\text{SD(Cont)}+\text{SD(Target)}]} - 2^{\text{AVE(Cont)}-\text{AVE(Target)}}}{\left[2^{\text{AVE(Cont)}-\text{AVE(Target)}}\right]_{\text{Neg}}} \quad (4.1)$$

where AVE and SD are the respective average and standard deviation of each quadruplicate sample, Cont and Target are the loading control and target, respectively, and Neg is the sample lacking a miRNA transfected with the same ligand concentration as the sample in question.

ACKNOWLEDGEMENTS

We thank A. Brown, Y.C. Chen, M. Greenwood-Goodwin, and J. Vowles for constructive comments on the manuscript and V.N. Kim for providing the pCK-Drosha-FLAG and pCK-DGCR8-FLAG plasmids. This work was supported by the Caltech Joseph Jacobs Institute for Molecular Engineering for Medicine (grant to C.D.S.), the Department of Defense (grant to C.D.S.), the National Institutes of Health (fellowship to K.G.H), and the National Science Foundation (fellowship to C.L.B.).

REFERENCES

Aagaard LA, Zhang J, von Eije KJ, Li H, Saetrom P, Amarzguioui M, Rossi JJ (2008) Engineering and optimization of the miR-106b cluster for ectopic expression of multiplexed anti-HIV RNAs. *Gene Ther* **15:** 1536-1549.

An CI, Trinh VB, Yokobayashi Y (2006) Artificial control of gene expression in mammalian cells by modulating RNA interference through aptamer-small molecule interaction. *RNA* **12:** 710-716.

Baek D, Villen J, Shin C, Camargo FD, Gygi SP, Bartel DP (2008) The impact of microRNAs on protein output. *Nature* **455:** 64-71.

Barrick JE, Breaker RR (2007) The distributions, mechanisms, and structures of metabolite-binding riboswitches. *Genome Biol* **8:** R239.

Bartel DP (2004) MicroRNAs: genomics, biogenesis, mechanism, and function. *Cell* **116:** 281-297.

Bartlett DW, Davis ME (2006) Insights into the kinetics of siRNA-mediated gene silencing from live-cell and live-animal bioluminescent imaging. *Nucleic Acids Res* **34:** 322-333.

Bauer M, Kinkl N, Meixner A, Kremmer E, Riemenschneider M, Forstl H, Gasser T, Ueffing M (2009) Prevention of interferon-stimulated gene expression using microRNA-designed hairpins. *Gene Ther* **16:** 142-147.

Bayer TS, Smolke CD (2005) Programmable ligand-controlled riboregulators of eukaryotic gene expression. *Nat Biotechnol* **23:** 337-343.

Beisel CL, Bayer TS, Hoff KG, Smolke CD (2008) Model-guided design of ligand-regulated RNAi for programmable control of gene expression. *Mol Syst Biol* **4:** 224.

Beisel CL, Smolke CD (2009) Design principles for riboswitch function. *PLoS Comput Biol* **5:** e1000363.

Berens C, Thain A, Schroeder R (2001) A tetracycline-binding RNA aptamer. *Bioorg Med Chem* **9:** 2549-2556.

Boudreau RL, Martins I, Davidson BL (2009) Artificial microRNAs as siRNA shuttles: improved safety as compared to shRNAs in vitro and in vivo. *Mol Ther* **17:** 169-175.

Boudreau RL, Monteys AM, Davidson BL (2008) Minimizing variables among hairpin-based RNAi vectors reveals the potency of shRNAs. *RNA* **14:** 1834-1844.

Cai X, Hagedorn CH, Cullen BR (2004) Human microRNAs are processed from capped, polyadenylated transcripts that can also function as mRNAs. *RNA* **10:** 1957-1966.

Desai SK, Gallivan JP (2004) Genetic screens and selections for small molecules based on a synthetic riboswitch that activates protein translation. *J Am Chem Soc* **126:** 13247-13254.

Dreyfus M, Regnier P (2002) The poly(A) tail of mRNAs: bodyguard in eukaryotes, scavenger in bacteria. *Cell* **111:** 611-613.

Ellington AD, Szostak JW (1990) In vitro selection of RNA molecules that bind specific ligands. *Nature* **346:** 818-822.

Friedman RC, Farh KK, Burge CB, Bartel DP (2009) Most mammalian mRNAs are conserved targets of microRNAs. *Genome Res* **19:** 92-105.

Gonzalez S, Castanotto D, Li H, Olivares S, Jensen MC, Forman SJ, Rossi JJ, Cooper LJ (2005) Amplification of RNAi--targeting HLA mRNAs. *Mol Ther* **11:** 811-818.

Gregory RI, Yan KP, Amuthan G, Chendrimada T, Doratotaj B, Cooch N, Shiekhattar R (2004) The Microprocessor complex mediates the genesis of microRNAs. *Nature* **432:** 235-240.

Grimm D, Streetz KL, Jopling CL, Storm TA, Pandey K, Davis CR, Marion P, Salazar F, Kay MA (2006) Fatality in mice due to oversaturation of cellular microRNA/short hairpin RNA pathways. *Nature* **441:** 537-541.

Guil S, Caceres JF (2007) The multifunctional RNA-binding protein hnRNP A1 is required for processing of miR-18a. *Nat Struct Mol Biol* **14:** 591-596.

Han J, Lee Y, Yeom KH, Kim YK, Jin H, Kim VN (2004) The Drosha-DGCR8 complex in primary microRNA processing. *Genes Dev* **18:** 3016-3027.

Han J, Lee Y, Yeom KH, Nam JW, Heo I, Rhee JK, Sohn SY, Cho Y, Zhang BT, Kim VN (2006) Molecular basis for the recognition of primary microRNAs by the Drosha-DGCR8 complex. *Cell* **125:** 887-901.

Han J, Pedersen JS, Kwon SC, Belair CD, Kim YK, Yeom KH, Yang WY, Haussler D, Blelloch R, Kim VN (2009) Posttranscriptional crossregulation between Drosha and DGCR8. *Cell* **136:** 75-84.

He L, He X, Lim LP, de Stanchina E, Xuan Z, Liang Y, Xue W, Zender L, Magnus J, Ridzon D, Jackson AL, Linsley PS, Chen C, Lowe SW, Cleary MA, Hannon GJ (2007) A microRNA component of the p53 tumour suppressor network. *Nature* **447:** 1130-1134.

He L, Thomson JM, Hemann MT, Hernando-Monge E, Mu D, Goodson S, Powers S, Cordon-Cardo C, Lowe SW, Hannon GJ, Hammond SM (2005) A microRNA polycistron as a potential human oncogene. *Nature* **435:** 828-833.

Hermann T, Patel DJ (2000) Adaptive recognition by nucleic acid aptamers. *Science* **287:** 820-825.

Jenison RD, Gill SC, Pardi A, Polisky B (1994) High-resolution molecular discrimination by RNA. *Science* **263:** 1425-1429.

Kedde M, Strasser MJ, Boldajipour B, Oude Vrielink JA, Slanchev K, le Sage C, Nagel R, Voorhoeve PM, van Duijse J, Orom UA, Lund AH, Perrakis A, Raz E, Agami R (2007) RNA-binding protein Dnd1 inhibits microRNA access to target mRNA. *Cell* **131:** 1273-1286.

Kiga D, Futamura Y, Sakamoto K, Yokoyama S (1998) An RNA aptamer to the xanthine/guanine base with a distinctive mode of purine recognition. *Nucleic Acids Res* **26:** 1755-1760.

Koizumi M, Breaker RR (2000) Molecular recognition of cAMP by an RNA aptamer. *Biochemistry* **39:** 8983-8992.

Lee JF, Hesselberth JR, Meyers LA, Ellington AD (2004) Aptamer database. *Nucleic Acids Res* **32:** D95-100.

Lee Y, Ahn C, Han J, Choi H, Kim J, Yim J, Lee J, Provost P, Radmark O, Kim S, Kim VN (2003) The nuclear RNase III Drosha initiates microRNA processing. *Nature* **425:** 415-419.

Lee Y, Jeon K, Lee JT, Kim S, Kim VN (2002) MicroRNA maturation: stepwise processing and subcellular localization. *EMBO J* **21:** 4663-4670.

Lee Y, Kim VN (2007) In vitro and in vivo assays for the activity of Drosha complex. *Methods Enzymol* **427:** 89-106.

Lorsch JR, Szostak JW (1994) In vitro selection of RNA aptamers specific for cyanocobalamin. *Biochemistry* **33:** 973-982.

Mannironi C, Di Nardo A, Fruscoloni P, Tocchini-Valentini GP (1997) In vitro selection of dopamine RNA ligands. *Biochemistry* **36:** 9726-9734.

McBride JL, Boudreau RL, Harper SQ, Staber PD, Monteys AM, Martins I, Gilmore BL, Burstein H, Peluso RW, Polisky B, Carter BJ, Davidson BL (2008) Artificial miRNAs mitigate shRNA-mediated toxicity in the brain: implications for the therapeutic development of RNAi. *Proc Natl Acad Sci U S A* **105:** 5868-5873.

Muller M, Weigand JE, Weichenrieder O, Suess B (2006) Thermodynamic characterization of an engineered tetracycline-binding riboswitch. *Nucleic Acids Res* **34:** 2607-2617.

Ogawa A, Maeda M (2008) An artificial aptazyme-based riboswitch and its cascading system in E. coli. *Chembiochem* **9:** 206-209.

Osborne SE, Ellington AD (1997) Nucleic Acid Selection and the Challenge of Combinatorial Chemistry. *Chem Rev* **97:** 349-370.

Sachs AB, Varani G (2000) Eukaryotic translation initiation: there are (at least) two sides to every story. *Nat Struct Biol* **7:** 356-361.

Selbach M, Schwanhausser B, Thierfelder N, Fang Z, Khanin R, Rajewsky N (2008) Widespread changes in protein synthesis induced by microRNAs. *Nature* **455:** 58-63.

Stern P, Astrof S, Erkeland SJ, Schustak J, Sharp PA, Hynes RO (2008) A system for Cre-regulated RNA interference in vivo. *Proc Natl Acad Sci U S A* **105:** 13895-13900.

Suess B, Fink B, Berens C, Stentz R, Hillen W (2004) A theophylline responsive riboswitch based on helix slipping controls gene expression in vivo. *Nucleic Acids Res* **32:** 1610-1614.

Suess B, Hanson S, Berens C, Fink B, Schroeder R, Hillen W (2003) Conditional gene expression by controlling translation with tetracycline-binding aptamers. *Nucleic Acids Res* **31:** 1853-1858.

Suess B, Weigand JE (2008) Engineered riboswitches: overview, problems and trends. *RNA Biol* **5:** 24-29.

Sun D, Melegari M, Sridhar S, Rogler CE, Zhu L (2006) Multi-miRNA hairpin method that improves gene knockdown efficiency and provides linked multi-gene knockdown. *Biotechniques* **41:** 59-63.

Thompson KM, Syrett HA, Knudsen SM, Ellington AD (2002) Group I aptazymes as genetic regulatory switches. *BMC Biotechnol* **2:** 21.

Tuerk C, Gold L (1990) Systematic evolution of ligands by exponential enrichment: RNA ligands to bacteriophage T4 DNA polymerase. *Science* **249:** 505-510.

Tuerk C, MacDougal S, Gold L (1992) RNA pseudoknots that inhibit human immunodeficiency virus type 1 reverse transcriptase. *Proc Natl Acad Sci U S A* **89:** 6988-6992.

Weigand JE, Sanchez M, Gunnesch EB, Zeiher S, Schroeder R, Suess B (2008) Screening for engineered neomycin riboswitches that control translation initiation. *RNA* **14:** 89-97.

Wilson C, Nix J, Szostak J (1998) Functional requirements for specific ligand recognition by a biotin-binding RNA pseudoknot. *Biochemistry* **37:** 14410-14419.

Win MN, Smolke CD (2007) A modular and extensible RNA-based gene-regulatory platform for engineering cellular function. *Proc Natl Acad Sci U S A* **104:** 14283-14288.

Xia XG, Zhou H, Xu Z (2006) Multiple shRNAs expressed by an inducible pol II promoter can knock down the expression of multiple target genes. *Biotechniques* **41:** 64-68.

Yen L, Svendsen J, Lee JS, Gray JT, Magnier M, Baba T, D'Amato RJ, Mulligan RC (2004) Exogenous control of mammalian gene expression through modulation of RNA self-cleavage. *Nature* **431:** 471-476.

Zeng Y, Cullen BR (2003) Sequence requirements for micro RNA processing and function in human cells. *RNA* **9:** 112-123.

Zeng Y, Cullen BR (2004) Structural requirements for pre-microRNA binding and nuclear export by Exportin 5. *Nucleic Acids Res* **32:** 4776-4785.

Zeng Y, Cullen BR (2005) Efficient processing of primary microRNA hairpins by Drosha requires flanking nonstructured RNA sequences. *J Biol Chem* **280:** 27595-27603.

Zeng Y, Wagner EJ, Cullen BR (2002) Both natural and designed micro RNAs can inhibit the expression of cognate mRNAs when expressed in human cells. *Mol Cell* **9:** 1327-1333.

Zeng Y, Yi R, Cullen BR (2005) Recognition and cleavage of primary microRNA precursors by the nuclear processing enzyme Drosha. *EMBO J* **24:** 138-148.

Zimmermann GR, Wick CL, Shields TP, Jenison RD, Pardi A (2000) Molecular interactions and metal binding in the theophylline-binding core of an RNA aptamer. *RNA* **6:** 659-667.

SUPPLEMENTARY INFORMATION

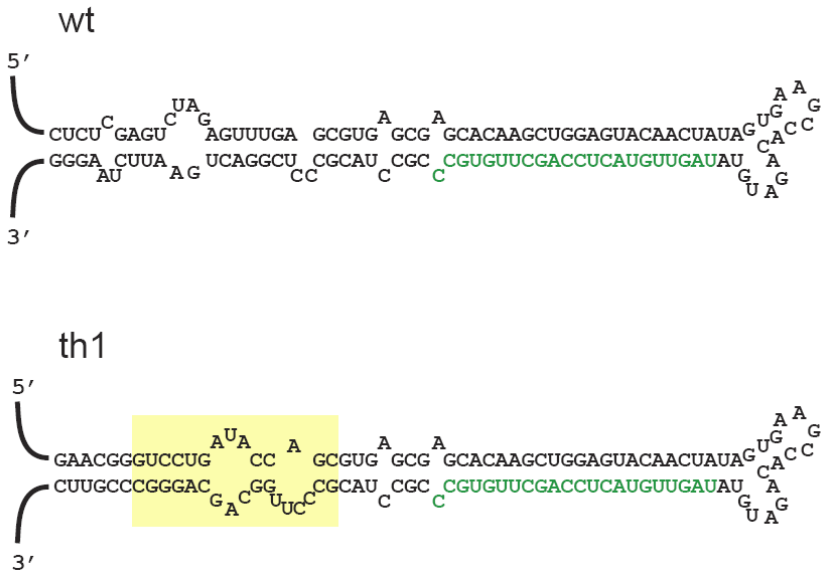

Figure S4.1 Sequence and secondary structures of miRNAs targeting GFP. Basal segments contain sequences that are similar to miR-30a (wt) or the theophylline aptamer (th1). The aptamer insertion site is indicated by the yellow box according to Figure 4.3A and the mature miRNA sequence complementary to the GFP transcript is indicated in green text.

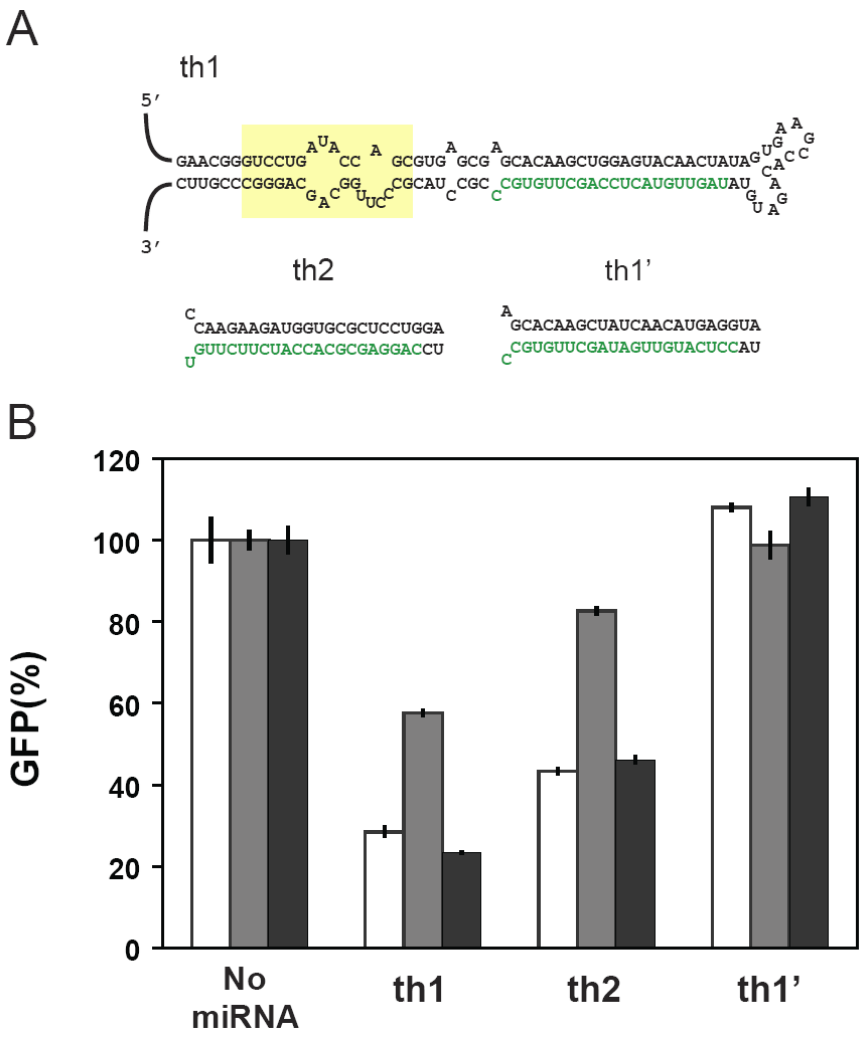

Figure S4.2 Ligand-responsive miRNAs can accommodate different mature miRNA sequences to tailor the gene silencing output of the regulatory system. (**A**) The mature miRNA sequence contained within the upper stem of th1 was modified to target a different sequence within the GFP mRNA (th2) or abolish targeting (th1’). All miRNAs contain the theophylline aptamer in the basal segments. The aptamer insertion site is indicated by the yellow box according to Figure 4.3A, and mature miRNA sequences are indicated in green text. The GFP-targeting miRNAs were cloned into the plasmid constructs and characterized through the cell culture assays described in Figure 4.1D. (**B**) GFP silencing results for theophylline-responsive miRNA constructs (th1, th2, or th1’) transiently transfected in the absence (white) or presence of either 5

mM theophylline (gray) or 1 mM caffeine (black). The population median of GFP fluorescence from transiently transfected HEK 293 cells stably expressing GFP was normalized to that from a construct lacking a miRNA (No miRNA) transfected under the same conditions. Error bars represent the standard deviation of two independent transfections.

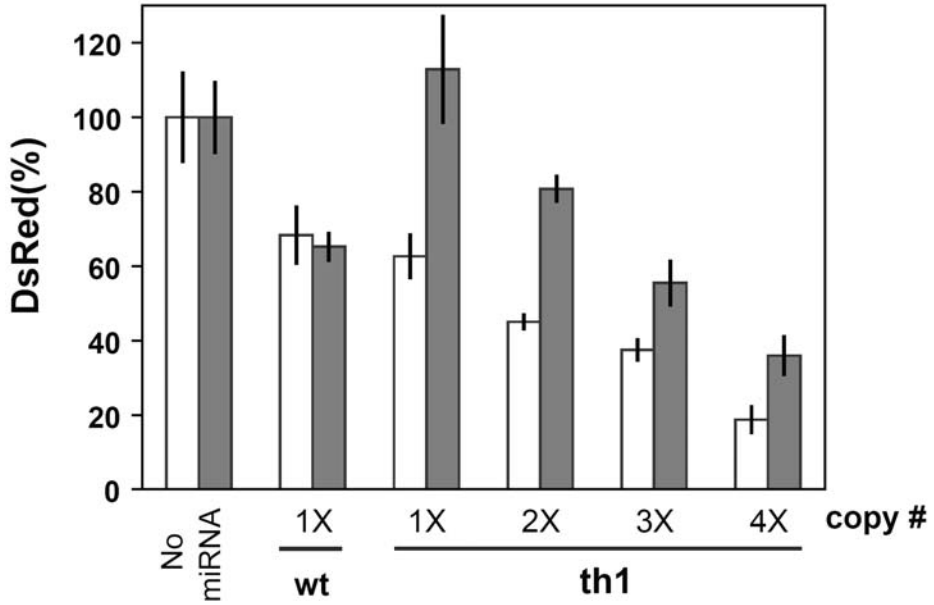

Figure S4.3 Ligand-responsive miRNAs control gene expression in cis through transcript destabilization. Multiple copies (#X) of the GFP-targeting (th1) theophylline-responsive miRNAs were cloned into the plasmid constructs described in Figure 4.1D using the largest spacer length tested (112 nt). wt was used as a negative control to allow direct comparison to Figure 4.4B. HEK 293 cells stably expressing GFP were transiently transfected with these constructs in the presence (gray) or absence (white) of 5 mM theophylline. DsRed transcript levels were measure through qRT-PCR and normalized to transcript levels of the Neomycin resistance gene expressed from the same transfected plasmid. Relative levels were normalized to that of cells transfected with the construct lacking any miRNAs (No miRNA) grown under the same conditions. Error bars represent the calculated error of quadruplicate qRT-PCR wells for each sample.

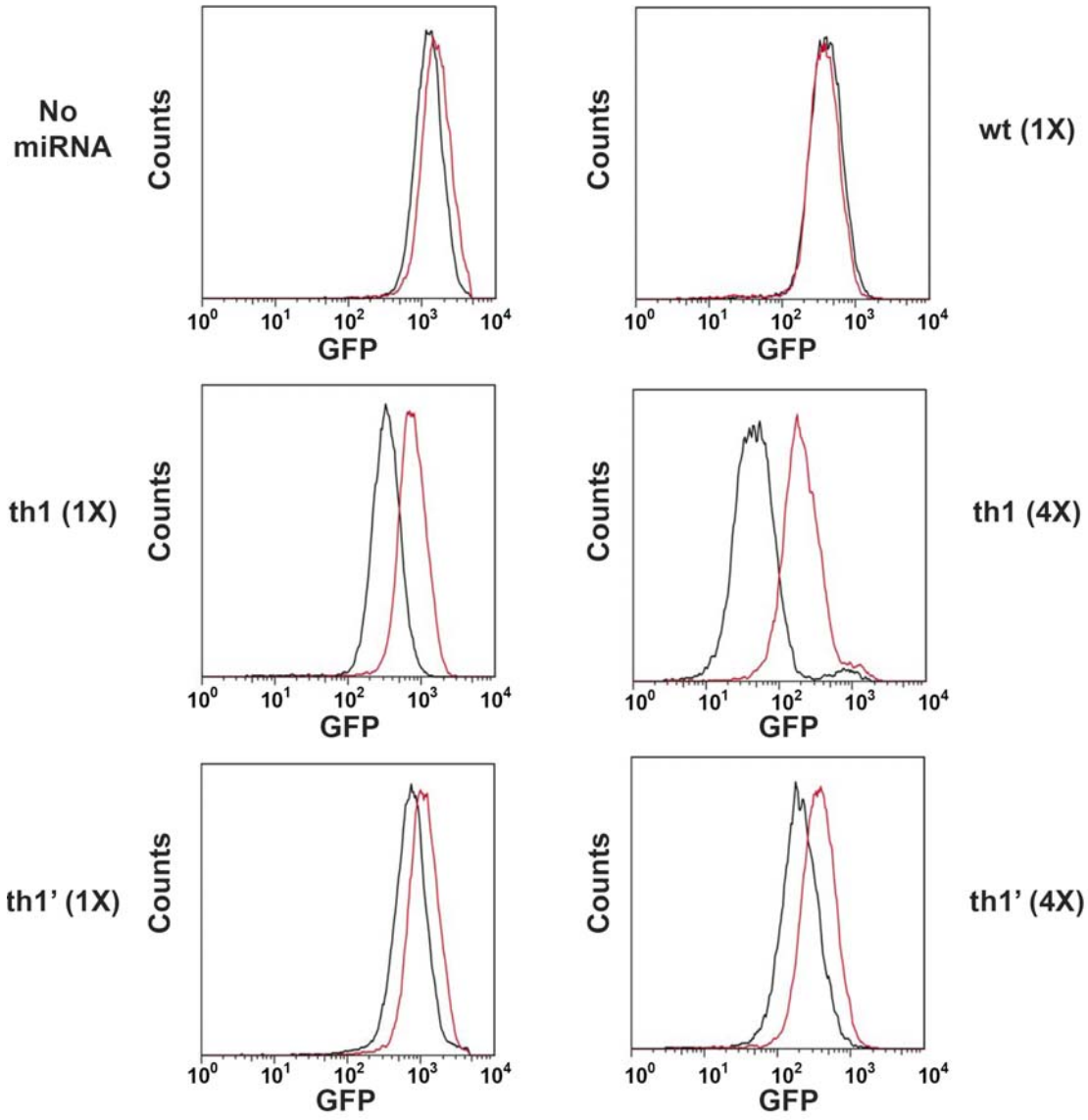

Figure S4.4 Flow cytometry histograms for HEK 293-Flp-In cells stably expressing the self-targeting miRNA constructs. miRNAs were located in the 3' UTR of the trans-targeted transcript encoding GFP. Constructs harboring no miRNAs (No miRNA), one copy of a self-targeting miRNA with basal segments containing sequences similar to miR-30a (wt), one (1X) or four (4X) copies of a theophylline-responsive self-targeting miRNA (th1), and one or four copies of a theophylline-responsive non-targeting miRNA (th1') were characterized, where multiple copies were separated by the largest spacer length tested (112 nt). Stable cell lines were grown for over

one week in the presence (red) or absence (black) of 1.5 mM theophylline prior to flow cytometry analysis.

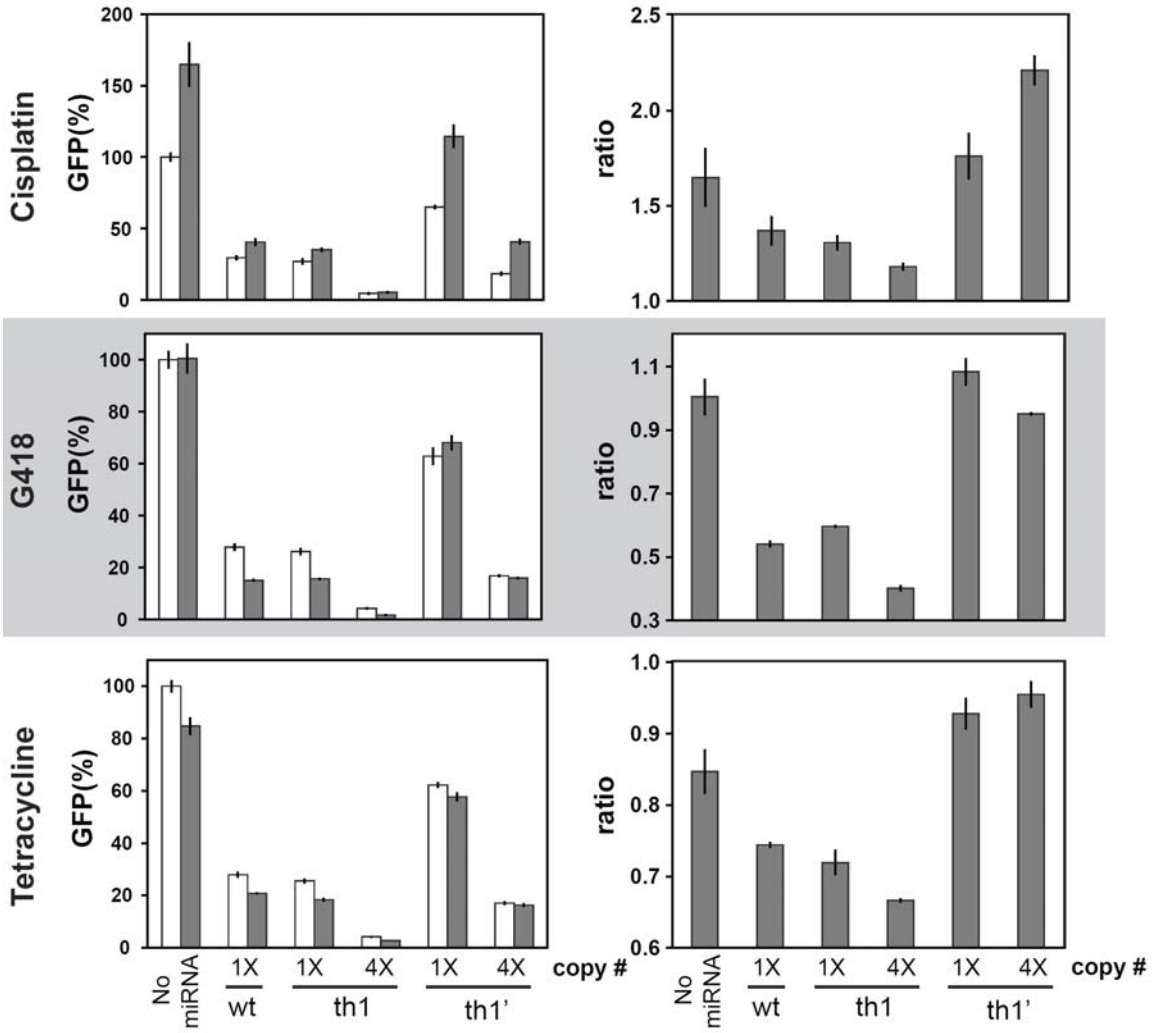

Figure S4.5 Self-targeting miRNAs confer differential response to cellular stress. miRNAs were located in the 3' UTR of the trans-targeted transcript encoding GFP. Constructs harboring no miRNAs (No miRNA), one copy of a self-targeting miRNA with basal segments containing sequences similar to miR-30a (wt), one (1X) or four (4X) copies of a theophylline-responsive self-targeting miRNA (th1), and one or four copies of a theophylline-responsive non-targeting miRNA (th1') were characterized, where multiple copies were separated by the largest spacer

length tested (112 nt). Stable cell lines were grown for over one week in the presence (gray) or absence (black) of 1 μg/ml cisplatin, 900 μg/ml G418, or 500 μM tetracycline prior to flow cytometry analysis. The right column reports the ratio of GFP levels in the presence and absence of theophylline. Error bars represent the standard deviation of cells grown in two separate culture wells.

Table S4.1 Sequences for ligand-responsive and control miRNAs. Each sequence is written 5' to 3' and represents the final construct cloned into XbaI and ApaI within pcDNA3.1(+). th3 was cloned into XhoI and XbaI in pcDNA3.1(+) already containing th1 to test the efficacy of two miRNAs separated by a minimal spacer. Color codes: gray, restriction sites; blue, aptamer; green, designed guide strand sequence. The database # is included for plasmid requests.

Name	Sequence	Aptamer	Database #
wt	TCTAGAGTTTGACAGTGAGCGAGCACAAGCTGGAGTACAACTATAGTGAAGCCACAGATGTATAGTTGTACTCCAGCTTGTGCCTGCCTACTGCCTCGGACTGAATTCATAGGGCCC	None	pCS351
m1	TCTAGAACGGGAAGTAATTACAGTGAGCGAGCACAAGCTGGAGTACAACTATAGTGAAGCCACAGATGTATAGTTGTACTCCAGCTTGTGCCTGCCTACTGCCACATAGGGCCC	None	pCS1246
m2	TCTAGAACGGGAAACACAGTGAGCGAGCACAAGCTGGAGTACAACTATAGTGAAGCCACAGATGTATAGTTGTACTCCAGCTTGTGCCTGCCTACTGCCTCGGGCCC	None	pCS1215
m3	TCTAGAACGGGAAACACAGTGAGCGAGCACAAGCTGGAGTACAACTATAGTGAAGCCACAGATGTATAGTTGTACTCCAGCTTGTGCCTGCCTACTGCCGGGCCC	None	pCS1241
m4	TCTAGAACGGGAAACACAGTGAGCGAGCACAAGCTGGAGTACAACTATAGTGAAGCCACAGATGTATAGTTGTACTCCAGCTTGTGCCTGCCTACTGGGGCCC	None	pCS1242

Table S4.1 cont'd

Name	Sequence	Aptamer	Database #
th1	TCTAGAACGGGTCCTGATACCAGCGTGAGCGAGCACAAGCTGGAGTACAACTATAGTGAAGCCACAGATGTATAGTTGTACTCCAGCTTGTGCCCGCCTACGCCCTTGGCAGCAGGGCCC	Theophylline	pCS1183
th1'	TCTAGAACGGGTCCTGATACCAGCGTGAGCGAGCACAAGCTATCAACATGAGGTAGTGAAGCCACAGATGTACCTCATGTTGATAGCTTGTGCCCGCCTACGCCCTTGGCAGCAGGGCCC		pCS1258
th2	TCTAGAACGGGTCCTGATACCAGCGTGAGCGCCAAGAAGATGGTGCGCTCCTGGAGTGAAGCCACAGATGTCCAGGAGCGCACCATCTTCTTGTCGCCTACGCCCTTGGCAGCAGGGCCC		pCS1664
th3	TCTAGACGCCAGAATGATACCAGCGTGAGCGAGCACAAGCTGGAGTACAACTATAGTGAAGCCACAGATGTATAGTTGTACTCCAGCTTGTGCCCGCCTACGCCCTTGGCAGCATTCTGGCGCCTAGG		pCS1229
tc1	TCTAGAACGGGTCCTAAAACATACCGTGAGCGAGCACAAGCTGGAGTACAACTATAGTGAAGCCACAGATGTATAGTTGTACTCCAGCTTGTGCCTGCCTACGGAGAGGTGAAGAATACGACCACCTAGGGCCC	Tetracycline	pCS1217
xa1	TCTAGAACGGGTCCGTGTATTACCTGAGCGAGCACAAGCTGGAGTACAACTATAGTGAAGCCACAGATGTATAGTTGTACTCCAGCTTGTGCCCGCCTAGGTCGACGGGCCC	Xanthine	pCS1218
xa2	TCTAGAACGGGTCCGAGGTCGACGTGAGCGAGCACAAGCTGGAGTACAACTATAGTGAAGCCACAGATGTATAGTTGTACTCCAGCTTGTGCCCGCCTACGTGTATTACCCAGGGCCC		pCS1244
La1	TCTAGAGTTTGACAGTGAGCGCTGGAAATCAGTGAAGATAAAATAGTGAAGCCACAGATGTATTTTATCTTCACTGATTTCCATTGCCTACTGCCTCGGACTGAATTCATAGGGCCC	None	pCS1676
La2	TCTAGAACGGGTCCTGATACCAGCGTGAGCGCTGGAAATCAGTGAAGATAAAATAGTGAAGCCACAGATGTATTTTATCTTCACTGATTTCCATCGCCTACGCCCTTGGCAGCAGGGCCC	Theophylline	pCS1677